

# Supporting Information

For

## Dynamic Morphologies of Microscale Droplet Interface Bilayers

P. Mruetusatorn,<sup>a</sup> J. B. Boreyko,<sup>c</sup> G. A. Venkatesan,<sup>b</sup> S. A. Sarles,<sup>b</sup>  
D. G. Hayes<sup>a</sup> and C. P. Collier<sup>\*c</sup>

<sup>a</sup>Department of Biosystems Engineering & Soil Science and <sup>b</sup>Department of Mechanical, Aerospace, and Biomedical Engineering, The University of Tennessee, Knoxville, Tennessee 37996, United States

<sup>c</sup>Center for Nanophase Materials Sciences, Oak Ridge National Laboratory, Oak Ridge, Tennessee 37831, United States

\*colliercp@ornl.gov

### Contents

#### Supplemental Figures

Fig. S1, S2	S2
Fig. S3, S4	S3
Movies of evaporating $\mu$ DIBs	S4

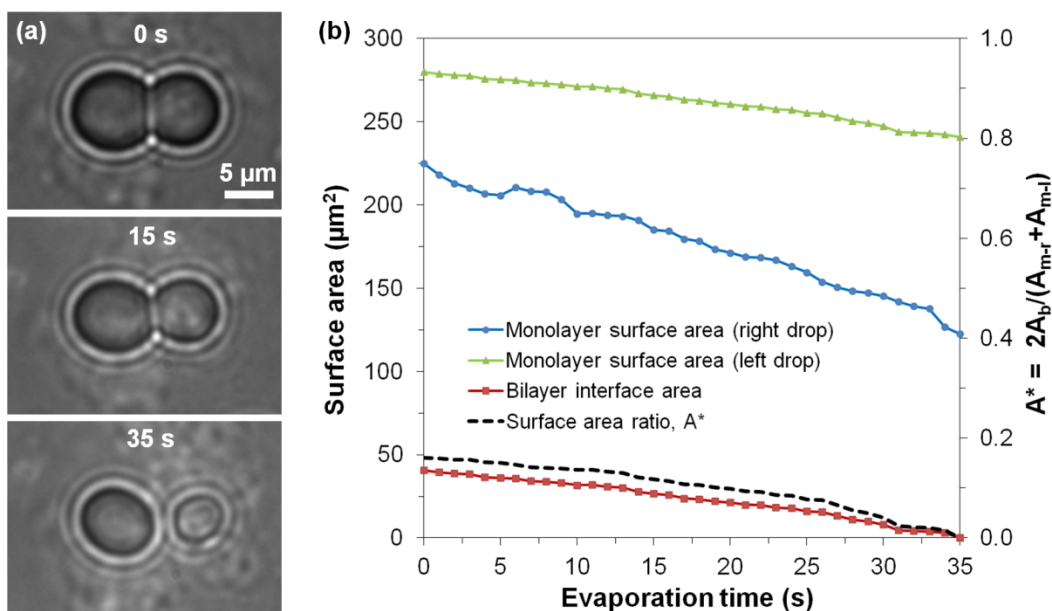


**Fig. S1** a) Additional experiment for a  $\mu$ DIB exhibiting stretching and unzipping to supplement Fig. 6. Both droplets were pinned due to lipid agglomerates. b) The right droplet shrinkage was over three times faster than the left droplet, due to a higher concentration of agglomerates at the right droplet's interface. See Movie M8 in Supporting Information.

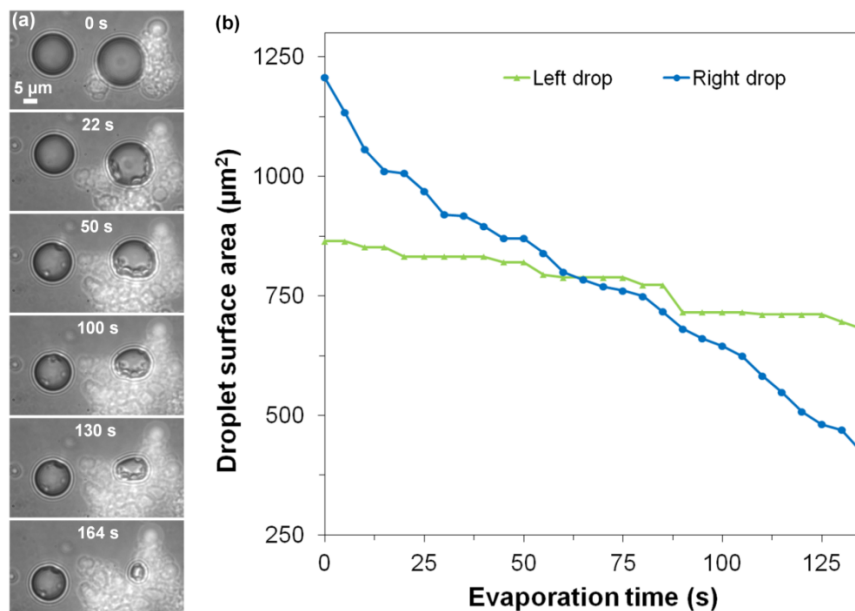


**Fig. S2** a) To verify that lipid agglomerates in the hexadecane locally accelerate the rate of droplet evaporation, two individual water droplets were observed with only the right droplet contacting agglomerates. b) Due to its contact with lipid agglomerates, the right droplet evaporated over four times faster than the left droplet. This confirms that the lipid agglomerates become hydrated by the water droplets. See Movie M9 in Supporting Information.

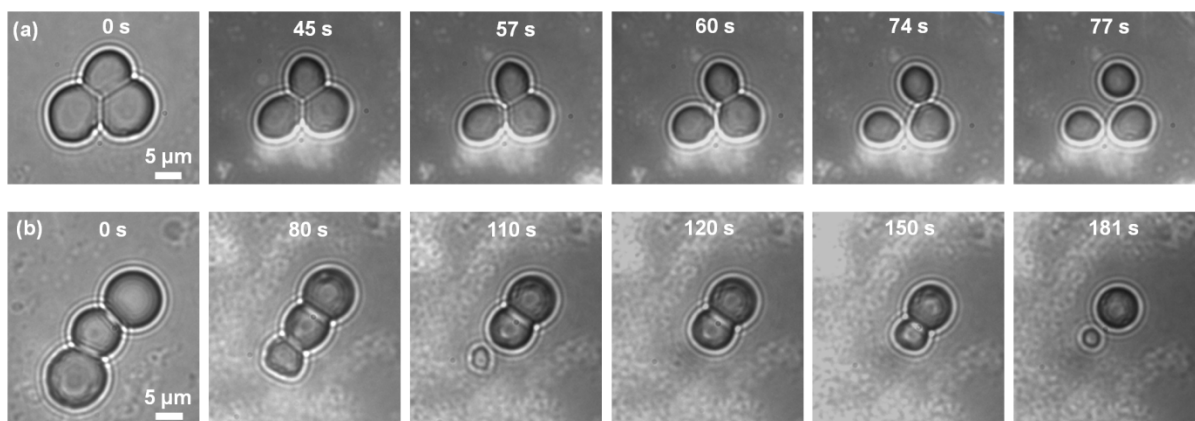


**Fig. S3** a) 3-droplet cluster and b) 3-droplet chain exhibiting stretching and unzipping. The white regions indicate the presence of lipid agglomerates. The droplet located around the most concentrated region of agglomerates is the first to separate from the droplet network, due to a faster evaporation rate and stronger pinning to the wall of the channel. See Movies M10 and M11 in Supporting Information.

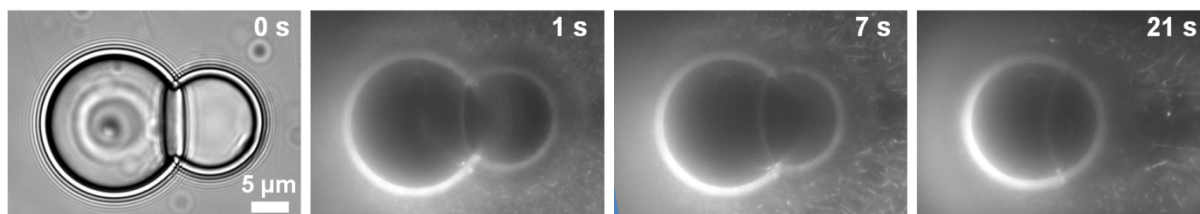


**Fig. S4** For the case of DOPC lipids dispersed in purified soybean oil, shape-change (into a single sphere) and buckling could still occur even when the droplets were wetting the walls. The wetting of the wall is indicated by the footprints of the droplets visible in bright-field, and fluorescent imaging was used to observe shape-change and buckling during evaporation. This indicates that wetting alone is not sufficient to cause stretching and unzipping type behavior; rather, the droplets need to be pinned to the wall. See Movie M12 in Supporting Information.

## **Movies of evaporating $\mu$ DIBs**

Prior to the recording of each movie, the microscope focus was adjusted until the maximal cross-section of the droplets/bilayers were in focus. The brightness and contrast were held constant throughout each movie. Movies M1-M12 were acquired at 1 FPS and played back at 20 FPS (20X fast forward), and Movie M13 was acquired at 0.1 FPS and played back at 25 FPS (250X fast forward).

**Movie M1.** 2-droplet buckling and fission (Fig. 1b). The field of view is  $32.4\ \mu\text{m} \times 32.4\ \mu\text{m}$ .

**Movie M2.** 3-droplet cluster exhibiting buckling (Fig. 3a). The field of view is  $32.4\ \mu\text{m} \times 32.4\ \mu\text{m}$ .

**Movie M3.** 5-droplet cluster exhibiting buckling (Fig. 3b). The field of view is  $45\ \mu\text{m} \times 55\ \mu\text{m}$ .

**Movie M4.** 10-droplet chain with buckling (Fig. 3c). The field of view is  $58.2\ \mu\text{m} \times 58.2\ \mu\text{m}$ .

**Movie M5.** 2-droplet uniform shrinking (Fig. 4b). The field of view is  $24\ \mu\text{m} \times 24\ \mu\text{m}$ .

**Movie M6.** 5-droplet cluster featuring uniform shrinking (Fig. 6). The field of view is  $40\ \mu\text{m} \times 40\ \mu\text{m}$ .

**Movie M7.** 2-droplet stretching and unzipping (Fig. 7b). The field of view is  $28\ \mu\text{m} \times 28\ \mu\text{m}$ .

**Movie M8.** Additional movie of 2-droplet stretching and unzipping (Fig. S1a). The field of view is  $32.4\ \mu\text{m} \times 32.4\ \mu\text{m}$ .

**Movie M9.** Accelerated droplet evaporation due to agglomerates (Fig. S2a). The field of view is  $50.4\ \mu\text{m} \times 40\ \mu\text{m}$ .

**Movie M10.** 3-droplet cluster exhibiting stretching and unzipping (Fig. S3a). The field of view is  $32.4\ \mu\text{m} \times 32.4\ \mu\text{m}$ .

**Movie M11.** 3-droplet chain exhibiting stretching and unzipping (Fig. S3b). The field of view is  $32.4\ \mu\text{m} \times 32.4\ \mu\text{m}$ .

**Movie M12.** 2-droplet  $\mu$ DIB wetting the wall but with negligible pinning effects exhibit buckling instead of stretching (Fig. S4). The field of view is  $32.4\ \mu\text{m} \times 32.4\ \mu\text{m}$ .

**Movie M13.** 2-droplet  $\mu$ DIB (left) and an isolated droplet (right) nucleated satellite water droplets at their interfaces due to the hydration of inverse micelles in the oil (Fig. 9). The field of view is  $228\ \mu\text{m} \times 168\ \mu\text{m}$ .